Thrust Force Ripple Minimization of Linear Flux-Switching PM Brushless AC Machines

Shigui Zhou, Haitao Yu, Minqiang Hu, Chongxue Jiang
Research Center for Motion Control of MOE, School of Electrical Engineering
Southeast University, Nanjing 210096, China
htyu@seu.edu.cn

Abstract —In this paper, the thrust force ripple of Linear Flux-Switching Permanent Magnet (LFSPM) machines is analyzed, and a novel LFSPM machine with less cogging force and optimal sinusoidal back-EMF is proposed. The method based on Fourier Algorithm is employed to reduce the cogging force due to slot-effect. In addiction, an optimal ratio of pole-width to pole-pitch for minimum harmonic components in the back-EMF is obtained by FE analysis. Finally, the proposed methods are validated by FE analysis and test.

I. INTRODUCTION

Linear Flux-Switching Permanent Magnet (LFSPM) machines have more advantages in reliability, manufacturing expenses and maintenance due to the magnets set on the short mover. However, the LFSPM machine suffers from severe thrust force ripples. In order to reduce it, various techniques in motor design or current control have been proposed [1][2][3].

II. THRUST FORCE RIPPLE OF LFSPM MACHINES

A. Topology of the LFSPM Machines

In Fig. 1a, τ_p is the pole pitch of stator, τ_{1t}=3/2τ_p is tooth pitch of each phase on the mover, and ρ=(6-1/3) τ_p is distance of two magnets of two adjacent phases. In addiction, the widths of teeth and poles are equal.

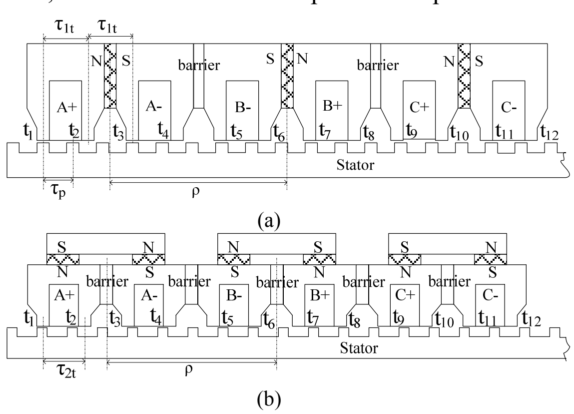

Fig. 1. Topology of the LFSPM motor. (a) current. (b) proposed.

B. Thrust Force Ripple Analysis

The thrust force of LFSPM machines can be expressed as follows

$$F_e = \frac{\partial}{\partial v}\left[\frac{1}{2}I^T LI + \psi_{pm}^T I\right] + F_{cog} = F_r + F_{pm} + F_{cog} \quad (1)$$

Assuming idealized sinusoidal back-EMF, and zero cogging force and zero reluctance force, ripple-free thrust force will be produced. Since the reluctance force can be neglected, the method for minimization of thrust force ripples can be summarized by the back-EMF waveform optimization and the cogging force minimization [4].

III. COGGING FORCE MINIMIZATION

A. Cogging Force of a LFSPM Machine

For simplification, the assumptions are made that the end effects are negligible and the core permeance is infinite. Thus, the study of the cogging force is reduced to the analysis of one of interactions between stator teeth and mover poles, considering each of them independently from the others [5][6]. The cogging force of one-tooth model can be described using a Fourier series expansion as

$$f(x) = \sum_{k=1}^{\infty} A_k \sin(k\lambda x + \alpha_k) \quad (2)$$

where $\lambda=2\pi/\tau_p$, A_k and α_k are the magnitude and phase of kth harmonic component respectively.

In Fig. 1a, the current linear FSPM machine has 12 mover teeth. If the phase angle of tooth t_1 is zero, the phases of 12 teeth in electrical angle θ_i can be illustrated in Fig. 2a.

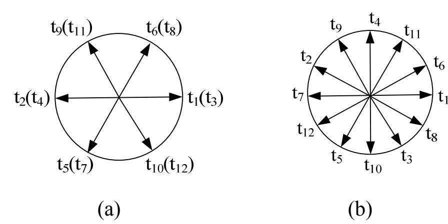

Fig. 2. Electrical angle distribution of tooth phase. (a) current. (b) proposed.

The cogging force of any tooth can be expressed as

$$f_i(x) = \sum_{k=1}^{\infty} A_k \sin[k(\lambda x + \theta_i) + \alpha_k] \quad (3)$$

So the total cogging force of the current linear FSPM machine is obtained

$$F_{cog}(x) = \sum_{i=1}^{12} f_i(x) = \sum_{i=1}^{12}\sum_{k=1}^{\infty} A_k \sin[k(\lambda x + \theta_i) + \alpha_k] \quad (4)$$

The kth harmonic component of the cogging force is

$$F_{cog}^{(k)}(x) = A_k \sum_{i=1}^{12} \sin[(k\lambda x + \alpha_k) + k\theta_i] = \begin{cases} 0 & k = 2n-1 \\ 0 & k = 2n, k \neq 6n \\ 12A_k \sin(k\lambda x + \alpha_k) & k = 6n, n = 1,2,3\cdots \end{cases} \quad (5)$$

B. Minimization of cogging force

The modifications for reduction cogging force are made as follows: 1) The distance between the adjacent mover tooth tips is changed into τ_{2t} = (3/2-1/12) τ_p. 2) The magnet of each phase is cut into two exact halves which are positioned on the top of corresponding stacks (Considering of the iron saturation and ensuring the equivalency of permeances of all the mover teeth).

The topology of the proposed LFSPM machine is shown in Fig. 1b, and the tooth phase distribution is changed as Fig. 2b. In the same way, the kth cogging force harmonic component of the proposed machine is

$$F_{cog}^{(k)}(x)=\begin{cases}0 & k=2n-1\\ 0 & k=2n, k\neq 12n\\ 12A_k\sin(k\lambda x+\alpha_k) & k=12n, n=1,2,3\cdots\end{cases} \tag{6}$$

Only 12 times order harmonic components are nonzero, the cogging force is reduced and been minimum.

The comparison of the cogging force between the current and proposed LFSPM machines by FE analysis is shown in Fig. 3a, and the measured waveform of the current LFSPM machine is shown in Fig. 3b.

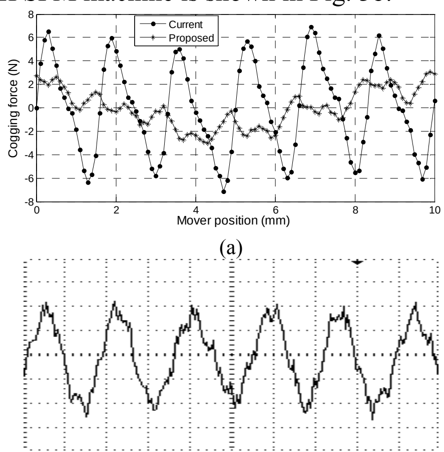

(a)

(b)

Fig. 3. Cogging force. (a) FE. (b) measured (4N/div, 10ms/div, 0.1m/s).

IV. BACK-EMF WAVEFORM OPTIMIZATION

In order to estimate the back-EMF waveform, the coefficient of the wave shape is defined that

$$C_e=\sum_{i=2}^{n}E_i^2\Big/E_1^2 \tag{7}$$

where E_i is the magnitude of the ith-order back-EMF harmonic component. The ratio of pole-width to pole-pitch of the stator is defined that

$$\alpha = w_p/\tau_p \tag{8}$$

Fig. 4 shows the profile of C_e and the magnitudes of back-EMF predicted by FE when α is varied from 0.1 to 0.9. thus, the width of pole changed from 0.45 to 0.4.

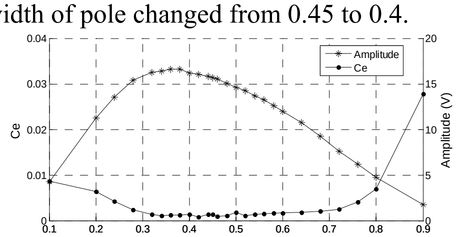

Fig. 4. Comparison of back-EMF

Fig. 5a shows the Back-EMF waveform comparison between the current machine with α=0.45 and proposed machine with α=0.4, and the measured waveform of the current LFSPM machine is shown in Fig. 5b.

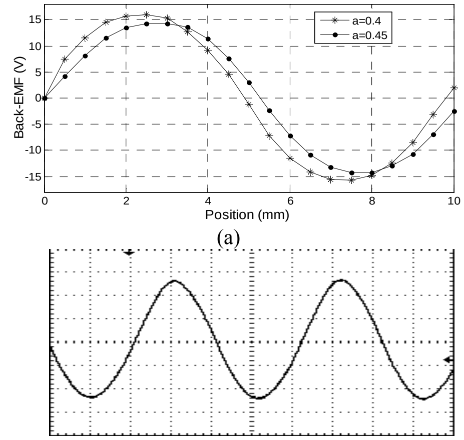

(a)

(b)

Fig. 5. Back-EMF waveform. (a) FE. (b) measured (5V/div, 5ms/div).

V. COMPARISON OF THRUST FORCE RIPPLE

When both the current and proposed LFSPM machines are fed 50Hz AC current resource on self-control model, the comparison of thrust force of two kinds of machines is shown in Fig. 6.

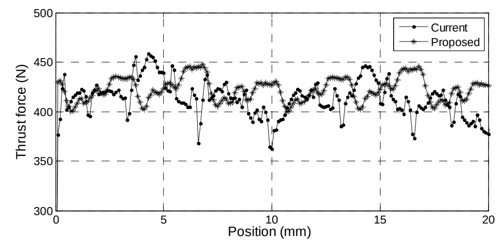

Fig.6. Comparison of thrust force by FE analysis (10A,50Hz, 0.5m/s).

VI. CONCLUTION

The thrust force ripple of the current LFSPM machine is analyzed, and a proposed machine with less cogging forces and optimal sinusoidal back-EMF is designed. Moreover, the proposed method is verified by FEA and test.

VII. REFERENCES

[1] Z. Zhu, A. Thomas, J. Chen, G. Jewell, “Cogging Torque in Flux-Switching Permanent Magnet Machines,” IEEE Trans. Magn., vol.45, no.10, pp.4708-4711, 2009.

[2] C. Wang, J. Shen, Y. Wang, L. Wang, M. Jin, “A New Method for Reduction of Detent Force in Permanent Magnet Flux-Switching Linear Motors,” IEEE Trans. Magn., vol.45, no.6, pp.2843-2846, 2009.

[3] H. Jia, M. Cheng, W. Hua, W. Zhao, W. Li, “Torque Ripple Suppression in Flux-Switching PM Motor by Harmonic Current Injection Based on Voltage Space-Vector Modulation,” IEEE Trans. Magn., vol.46, no.6, pp.1527-1530, 2010.

[4] W. Hua, M. Cheng, Z. Zhu, D. Howe, “Analysis and Optimization of Back EMF Waveform of a Flux-Switching Permanent Magnet Motor,” IEEE Trans. Ener. Conv., vol.23, no.3, pp.727-733, 2008.

[5] S. Youn, J. Lee, H. Yoon, C. Koh, “A New Cogging-Free Permanent-Magnet Linear Motor,” IEEE Trans. Magn., vol.44, no.7, pp.1785-1790, 2008.

[6] N. Bianchi, S. Bolognani, “Design Techniques for Reducing the Cogging Torque in Surface-Mounted PM Motors,” IEEE Trans. Magn., vol.38, no.5, pp.1259-1265, 2002.